chemistry

MDPI

Article

Novel Ansa-Chain Conformation of a Semi-Synthetic Rifamycin Prepared Employing the Alder-Ene Reaction: Crystal Structure and Absolute Stereochemistry †

Christopher S. Frampton [1,*], James H. Gall [2] and David D. MacNicol [2,*]

[1] Experimental Techniques Centre, Brunel University London, Kingston Road, Uxbridge, Middlesex UB8 3PH, UK
[2] School of Chemistry, University of Glasgow, Glasgow G12 8QQ, UK; james.gall@glasgow.ac.uk
* Correspondence: chris.frampton@brunel.ac.uk (C.S.F.); david.macnicol@glasgow.ac.uk (D.D.M.); Tel.: +44-7841-373969 (C.S.F.)
† Dedicated to Dr. Howard Flack (1943–2017).

Abstract: Rifamycins are an extremely important class of antibacterial agents whose action results from the inhibition of DNA-dependent RNA synthesis. A special arrangement of unsubstituted hydroxy groups at C21 and C23, with oxygen atoms at C1 and C8 is essential for activity. Moreover, it is known that the antibacterial action of rifamycin is lost if either of the two former hydroxy groups undergo substitution and are no longer free to act in enzyme inhibition. In the present work, we describe the successful use of an Alder-Ene reaction between Rifamycin O, **1** and diethyl azodicarboxylate, yielding **2**, which was a targeted introduction of a relatively bulky group close to C21 to protect its hydroxy group. Many related azo diesters were found to react analogously, giving one predominant product in each case. To determine unambiguously the stereochemistry of the Alder-Ene addition process, a crystalline zwitterionic derivative **3** of the diethyl azodicarboxylate adduct **2** was prepared by reductive amination at its spirocyclic centre C4. The adduct, as a mono chloroform solvate, crystallized in the non-centrosymmetric Sohnke orthorhombic space group, $P2_12_12_1$. The unique conformation and absolute stereochemistry of **3** revealed through X-ray crystal structure analysis is described.

Keywords: Rifamycin O; ansamysin; antibacterial; semi-synthesis; Alder-Ene; conformation; zwitterionic; hydrogen bonding; absolute configuration; chirality; crystal structure; X-ray crystallography

Citation: Frampton, C.S.; Gall, J.H.; MacNicol, D.D. Novel Ansa-Chain Conformation of a Semi-Synthetic Rifamycin Prepared Employing the Alder-Ene Reaction: Crystal Structure and Absolute Stereochemistry . *Chemistry* **2021**, *3*, 734–743. https://doi.org/10.3390/chemistry3030052

Academic Editors: Catherine Housecroft and Katharina M. Fromm

Received: 26 May 2021
Accepted: 9 July 2021
Published: 11 July 2021

1. Introduction

The rifamycins constitute an important class of ansamycin antibiotic active against mycobacteria and other bacterial pathogens, also exhibiting antiviral properties. These molecules are comprised of a substituted naphthalene or naphthoquinone core spanned by a seventeen-membered aliphatic ansa bridge. A vast number of semi-synthetic rifamycins have been produced by structural modification of the aromatic region of naturally occurring rifamycins [1]. The important bridging ansa moiety has not been so intensively studied, though recent highlights are the excellent antibacterial activity found for 24-desmethylrifampicin [2]; and the synthesis of C25 carbamate derivatives which are resistant to ADP-ribosyl transferases [3]. The present work was directed at the introduction of a bulky group close to the hydroxy group on C21 of Rifamycin O, **1**, Scheme 1, to inhibit transferase deactivation [4,5]. Attempts to carry out a Diels–Alder reaction with dimethyl acetylenedicarboxylate, hoping to exploit the *cisoid* diene arrangement of **1**, torsion angle 36°, in the crystal [6] proved unsuccessful; however, gratifyingly, we found that diethyl azodicarboxylate and related diesters reacted readily and quantitatively giving a major product, along with a by-product in each case. The disappearance of a methyl doublet from the proton NMR spectrum with introduction of an allylic methyl singlet at lower field (see

methyl assignments in Experimental) clearly pointed to an Alder-Ene reaction [7,8] rather than a Diels–Alder reaction for which four methyl doublets would have been expected. MS confirmed a 1:1 adduct had been formed and inspection of a tactile Dreiding model of 1 revealed that azo nitrogen attack at the C18 alkene face giving an *S* configuration at C18 would, to effect hydrogen abstraction from C20, lead to a *trans* (*E*) double bond between C19 and C20. Corresponding alternative attack on the opposite alkene face would lead to an *R* configuration at the C18 stereogenic centre with a predicted *cis (Z)* double bond formed between C19 and C20. Although product **2** was obtained stereochemically pure at C4 (single AB quartet for the diastereotopic methylene protons of the spirolactone at C4), suitable single crystals for X-ray analysis could not be obtained. However, crystals were obtained from chloroform for **3**, which was derived from **2** by reductive amination as described in the Experimental section below and this resolved the stereochemical question and also revealed an unprecedented ansa-chain conformation.

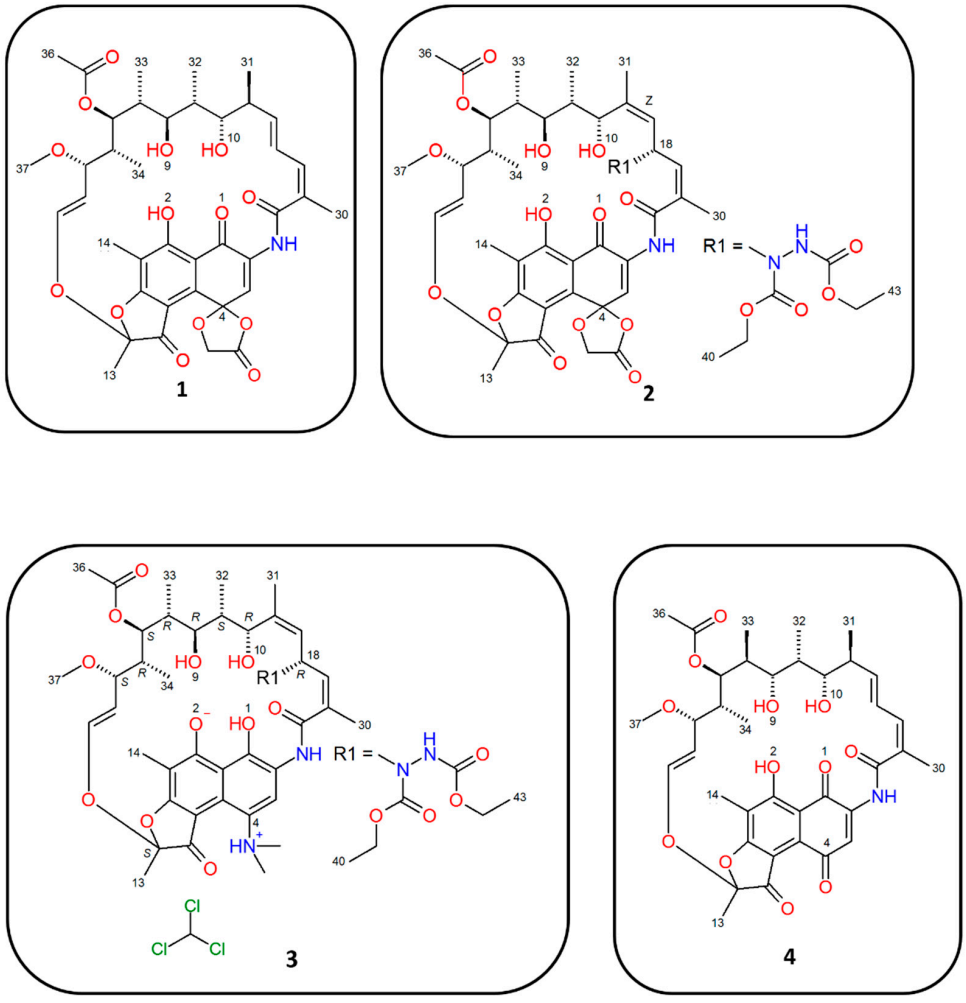

Scheme 1. Rifamycin structures referred to in the text.

2. Materials and Methods

Typical reaction conditions for **2**: compound **1** (1g, 0.00132 mmol) and diethyl azodicarboxylate (0.69 g, 0.00396 mmol) were refluxed in toluene (40 mL) under argon for 5 h and then left at 50 °C for one week. The toluene was removed, and the reaction product boiled in iso-propanol and then cooled and filtered, yielding **2** as a yellow powder. Assignments for the methyl resonances of **2**: ^{1}HNMR (400 MHz, $CDCl_3$), δ_H, C34, 0.16, 3H, *d*, *J* = 7 Hz; C33, 0.60, 3H, *d*, *J* = 7 Hz; C32, 1.02, 3H, *d*, *J* =7 Hz; C40 or C43, 1.22, 3H, *t*, *J* = 7 Hz; C40 or C43, 1.28, 3H, *t*, *J* = 7 Hz; C13, 1.68, 3H, s; C31, 1.77, 3H, *s*; C30,1.96, 3H, *s*; C36, 2.06,

3H, s; C14, 2.20, 3H, *s*; C37, 3.06, 3H, *s*. It may be noted that the spectrum, relevant to a future analysis of the conformational situation in solution, not considered here, shows retention of all functional groups including the unaltered (*E*) vinyl ether bridge component. Dimethyl azodicarboxylate and related, di*iso*propyl and dibenzyl esters, for example, all exhibited similar reactivity with respect to the Alder-Ene reaction with Rifamycin O **1**. The Alder-Ene reactions were quantitative, a single minor by-product being formed in each case; typical ratios being approximately 5:1. ^{1}HNMR data were collected on a Bruker AV III 400 MHz spectrometer.

Compound **2** was converted with modest yield into **3** by employing the general reductive amination procedure of Cricchio and Tamborini as described in [9], in which, interestingly, the amine acts a reducing agent. An excess of dimethylamine methanol solution was added by syringe to compound **2** in dry degassed THF and this was then left in the dark at 50 °C for a week. The THF was removed and the reaction product was dissolved in ethyl acetate and shaken with 7.4 pH phosphate buffer. The acetate layer was washed with water, dried, and the solvent evaporated to give **3**. Crystallisation of **3** proved challenging. However, small colourless single crystals of a plate morphology suitable for X-ray analysis were obtained from a $CHCl_3$ solution.

X-ray intensity data for **3** were collected at 100(1)K on a Rigaku Oxford Diffraction SuperNova Dual-flex AtlasS2 diffractometer equipped with an Oxford Cryosystems Cobra cooler using Cu $K\alpha$ radiation (λ = 1.54178 Å). The crystal structure was solved with SHELXT-2018/2 [10] and refined with SHELXL-2018/3 [11]. Hydrogen atoms bound to carbon were placed at geometrically calculated positions with $C_{methine}$-H = 1.00 Å, $C_{methylene}$-H = 0.99 Å, C_{methyl}-H = 0.98 Å, $C_{aromatic}$-H = 0.95 Å. These hydrogen atom positions were refined using a riding model with U_{iso}(H) = 1.2 U_{eq} (C) (1.5 U_{eq} (C) for methyl groups). Methyl group torsion angles were allowed to refine whilst maintaining an idealized tetrahedral geometry. Heteroatom (N-H, O-H) hydrogen atoms were located via a difference Fourier synthesis and their positions and isotropic temperature factors were allowed to refine freely. Values of the Flack *x* parameter [12] were obtained from the final refinement cycle of SHELXL. Two values were calculated, the first using the TWIN and BASF instructions and the second using the Parsons method of Intensity Quotients [13]. The Hooft *y* parameter [14–16] was calculated through the implementation in the program PLATON [17]. Details of the sample, data collection and structure refinement are given in Table 1. Crystal packing and structural overlay figures were produced using the CCDC program Mercury [18].

Table 1. Sample, data collection and structure refinement for compound **3**.

	Compound 3
Empirical formula	$C_{45}H_{62}N_4O_{15}$, $CHCl_3$
M_r	1018.35
T (K)	100(1)
Wavelength	Cu$K\alpha$ (1.54178 Å)
Crystal system	Orthorhombic
Space group	$P2_12_12_1$
a (Å)	14.4057(4)
b (Å)	14.9409(3)
c (Å)	22.8735(7)
α (°)	90
β (°)	90
γ (°)	90
V, (Å^3)	4923.2(2)
Z', Z	1, 4
ρ_{calc} (Mg m^{-3})	1.374
μ (mm^{-1})	2.287

Table 1. *Conts.*

	Compound 3
$F(000)$	2152
Crystal colour, shape	Colourless, plate
Size (mm)	0.251 × 0.250 × 0.071
Diffraction limit	0.80 Å
Coverage, %	99.9
Friedel coverage, %	81.0
Friedel fraction max %	99.8
Reflections collected/unique	26,683/10,050
R_{int}	0.0406
Observed reflections, $I > 2\sigma(I)$	9228
$T_{min,}$ T_{max}	0.748, 1.000
Data/restraints/parameters	10,050/0/650
GOF, (S) on F^2	1.035
R_1 $[I > 2\sigma(I)]$	0.0422
wR^2 (all data)	0.1140
Flack x parameter (refined)	−0.003(18)
Flack x parameter (from 3814 quotients)	−0.009(9)
Hooft y parameter	−0.008(6)
Min/max residual density (e Å^{-3})	0.658/−0.481
CCDC deposition number	2,045,594

CCDC 2045594 contains the supplementary crystallographic data for compound **3**, which can be obtained free of charge from The Cambridge Crystallographic Data Centre, see www.ccdc.cam.ac.uk/structures.

3. Results

Small colourless crystals of **3** exhibiting a plate morphology were obtained from slow evaporation of a chloroform solution. The asymmetric unit of the structure consists of a single fully ordered molecule of compound **3** and a single fully ordered molecule of chloroform as a solvate. The structure refined very well in the non-centrosymmetric Sohnke orthorhombic space group, $P2_12_12_1$ and gave a final residual R-factor based on the observed data of R_1 $[I > 2\sigma(I)]$ = 4.22 %. Figure 1 shows the asymmetric unit viewed obliquely from below the plane of the basal naphthenic moiety. Figure 2 shows a view of molecule of compound **3** with -CH hydrogen atoms removed for clarity and intramolecular contacts as green dashed lines; this view is obliquely down onto the plane of the basal naphthenic moiety. Selected torsion angle and intermolecular contact distances are listed in Table 2 along with comparative data for Rifamycin O, **1** and Rifamycin S, **4** (CSD codes PUTDUD [1] and PAFRAP [19]). Geometric hydrogen bond data are given in Table 3. The structure is zwitterionic, reflecting the high acidity of the OH group on C8, see for example [20–22]. The substituted 1,2-Dihydro-naphtho[2,1-*b*]furan moiety defined by atoms C1 to C12, O3 is planar with an r.m.s. deviation of the fitted atoms of 0.0586 Å, with atom C2 showing the greatest deviation from planarity, −0.124(3) Å. The single chloroform solvate molecule in the symmetric unit forms two short C-H···O interactions of [H46···O1, 2.395 Å] and [H46···O14, 2.255 Å]. There is possibly a small rotational disorder component to the solvent molecule, as evidenced by the small difference density maxima located near the chlorine atoms.

Table 2. Selected torsion angles (°) and intramolecular contact distances (Å) for compound **3** and related structures *.

Torsion Angle	Compound 3	Rifamycin O PUTDUD, 1	Rifamycin S PAFRAP, 4
C2-N1-C15-C16	−173.29(3)	−176.4	−177.3
N1-C15-C16-C17	59.8(4)	63.6	92.8
O3-C12-O5-C29	−85.2(3)	−81.7	−61.6
C12-O5-C29-C28	66.0(4)	65.9	−117.2
C21-C22-C23-C24	55.0(4)	63.2	60.4
C20-C21-C22-C23	176.0(3)	−172.1	−174.8
C25-C26-C27-C28	−171.6(3)	56.0	−172.3
C16-C17-C18-C19	146.4(3)	36.5	178.8
C17-C18-C19-C20	−136.4(3)	−178.6	−175.3
C18-C19-C20-C21	−1.2(5)	117.4	−45.6
C19-C20-C21-C22	92.8(4)	172.5	−175.6
Intramolecular Contact Distance	**Compound 3**	**Rifamycin O PUTDUD, 1**	**Rifamycin S PAFRAP, 4**
O1⋯⋯O2	2.436(4)	2.538	2.566
O1⋯⋯O9	7.622(4)	4.300	7.245
O1⋯⋯O10	6.906(4)	2.912	6.205
O2⋯⋯O9	8.276(4)	3.613	6.166
O2⋯⋯O10	7.811(4)	3.980	7.836
O9⋯⋯O10	2.711(4)	2.702	2.689
C2⋯⋯C33	3.474(5)	6.601	6.314
C3⋯⋯C33	3.383(5)	6.442	5.858

* Structural data for Rifamycin O and Rifamycin S, CSD codes PUTDUD and PAFRAP are taken from [1] and [19], respectively.

Table 3. Intra and intermolecular hydrogen bond data (Å,°) *.

D-H⋯⋯A	*d*(D⋯⋯H)	*d*(H⋯⋯A)	*d*(D⋯⋯A)	<(DHA)
O1-H1A⋯⋯O2	0.96(8)	1.54(8)	2.436(3)	154(7)
O9-H9⋯⋯O4′	0.73(6)	2.10(6)	2.750(4)	149(6)
O10-H10⋯⋯O9	0.75(6)	2.04(6)	2.711(4)	148(6)
N1-H1B⋯⋯O1	0.89(5)	2.22(5)	2.666(4)	111(4)
N1-H1B⋯⋯O14	0.89(5)	2.54(5)	3.390(4)	159(4)
N1-H1A⋯⋯N2	0.89(5)	2.68(5)	3.279(4)	126(4)
N3-H3⋯⋯O11″	0.86(5)	1.94(5)	2.771(4)	163(4)
N4-H4⋯⋯O4	1.00(5)	1.60(5)	2.595(4)	171(4)

* Symmetry operations; $'-x, y-1/2, -z+1/2$, $''-x+1, y-1/2, -z+1/2$.

The packing of molecules in the crystal is governed by the formation of two intermolecular hydrogen bond interactions. The first interaction is a hydroxy hydrogen, -OH, acting as a donor to a furanone carbonyl oxygen atom acting as an acceptor [O9-H9⋯O4, 2.750(4) Å]. The second interaction is an amide hydrogen, -NH, acting as a donor to a carbonyl oxygen atom acting as an acceptor [N3-H3⋯O11, 2.771(4) Å]. Both interactions use the same 2_1 screw axis symmetry operation along the *b*-axis, the second interaction is translated by one-unit cell along the *a*-axis, thus linking the molecules into a crosslinked infinite chain parallel to the *b*-axis of the unit cell, as shown in Figure 3. Details of the hydrogen bond interactions are given in Table 3.

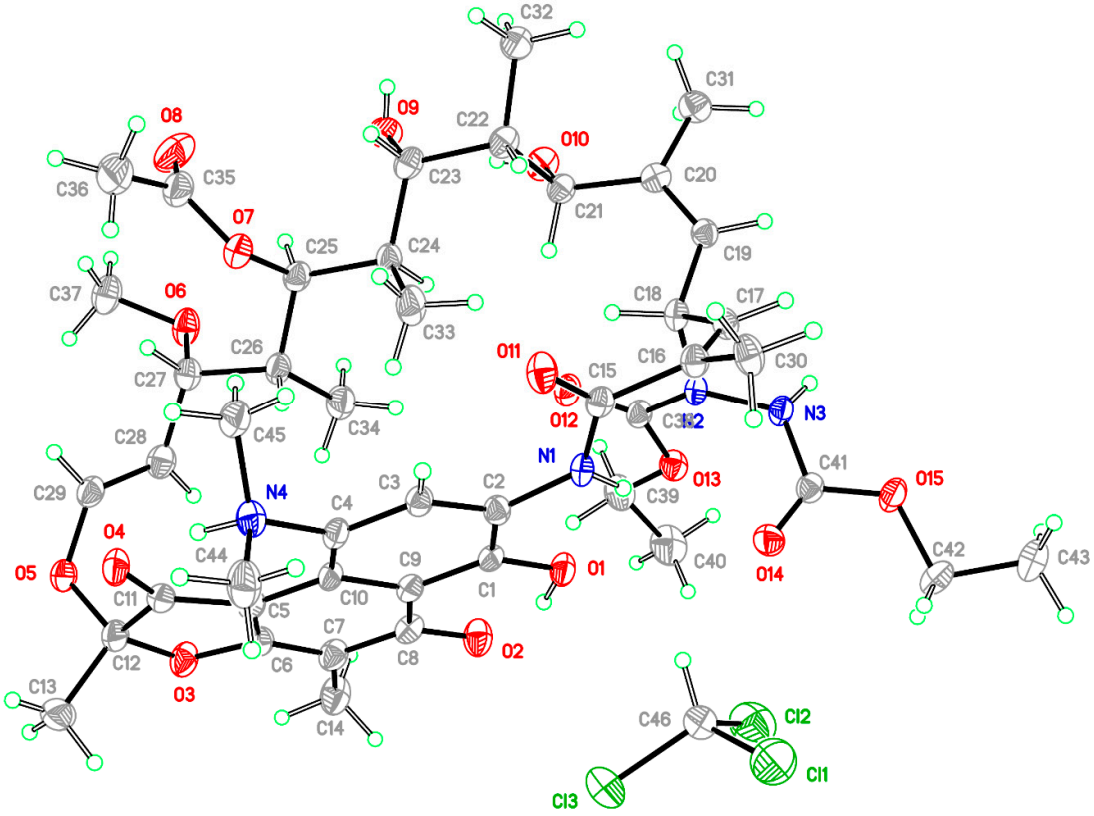

Figure 1. A view of the asymmetric unit of the crystal structure showing the atom numbering scheme employed. In this figure, the structure is viewed obliquely from below the naphthalene ring. Anisotropic atomic displacement ellipsoids for the non-hydrogen atoms are shown at the 50% probability level. Hydrogen atoms are displayed with an arbitrary small radius.

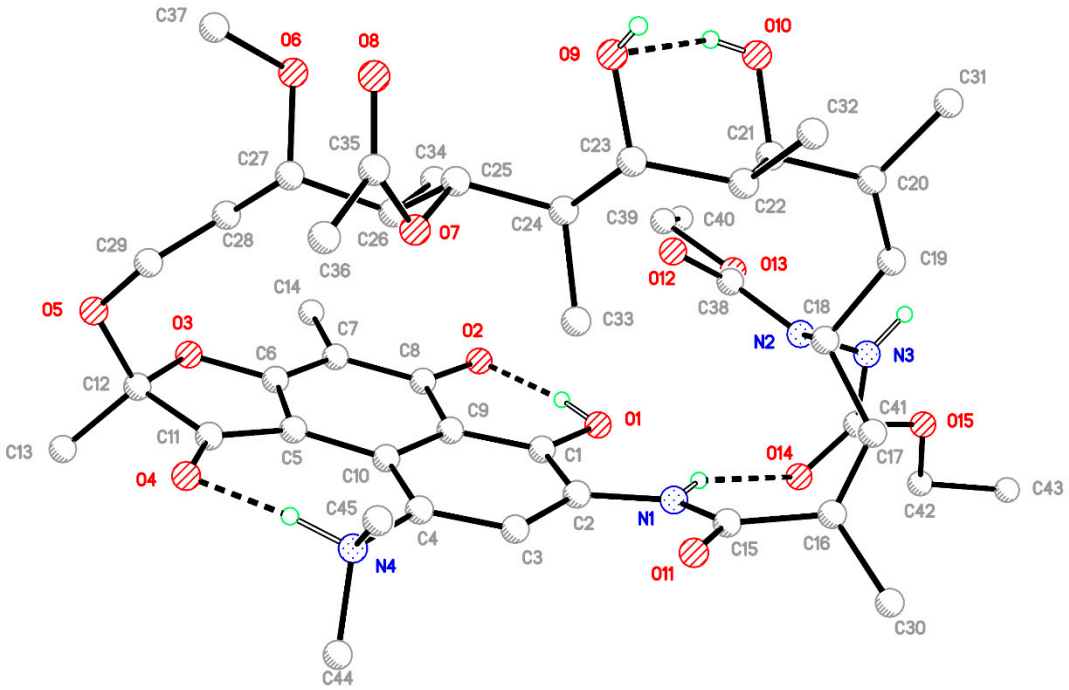

Figure 2. A view of a molecule of compound **3** from the crystal structure showing the atom numbering scheme employed and the intramolecular hydrogen bonds as dashed lines. In this figure, the structure is viewed obliquely from above the naphthalene ring. C-H hydrogen atoms have been removed for clarity.

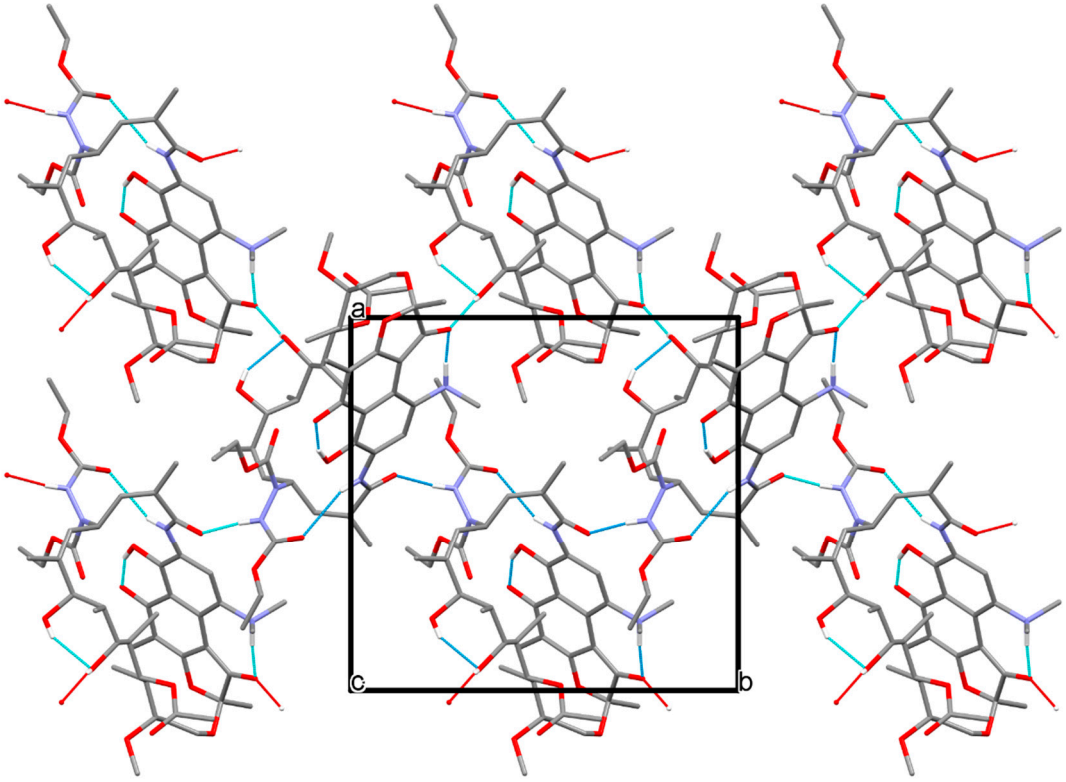

Figure 3. A view of part of the crystal packing of compound **3**, showing the formation of a layer of two crosslinked infinite chains parallel to the *b*-axis of the unit cell. Inter- and intramolecular hydrogen bond interactions are shown as dark and light blue dashed lines, respectively. Incomplete hydrogen bonds are shown as red dashed lines.

4. Discussion

The absolute stereochemistry of a single crystal of **3** has been determined through the anomalous dispersion effect on the diffracted beam intensities. This result was greatly enhanced by the fact that the crystal was a mono chloroform solvate since the anomalous scatting coefficients for the chlorine atoms are much larger than those for C, N and O for Cu *Kα* radiation. For the structure as presented with the chiral centres C12, C18, C21, C22, C23, C24, C25, C26, C27 in the *S*, *R*, *R*, *S*, *R*, *R*, *S*, *R*, *S* configuration, respectively, the Flack parameter = −0.003(18). Determination of the absolute structure using Bayesian statistics on Bijvoet differences (Hooft method), reveals that the probability of the absolute structure as presented being correct is 1.000, while the probabilities of the structure being a racemic twin or false are both 0.000. The Flack equivalent and its uncertainty calculated through this program was $y = -0.008(6)$. This calculation was based on the values of 4497 Bijvoet differences. The post refinement method based on 3814 intensity quotients (Parsons method) gave a value of $x = -0.009(9)$. It can be seen that all three methods are in good agreement (with the exception of the standard uncertainty value which is approximately a factor of two greater for the refined parameter) and that the absolute stereochemistry of compound **3** is well defined. As can be seen, the molecule has an *R* configuration at C18 and the introduced double bond between C19 and C20 has a *cis* (*Z*) configuration. Since **3** came directly from the pure major product of the Alder-Ene reaction, this establishes that the major product has the structure **2** as formulated. A salient feature is the wide separation of O1-O10 and of O2-O9, these distances having increased by 3.994 and 4.663 Å from those of Rifamycin O, **1**, in the crystal. Also striking is the location of the methyl group, (C33), attached to C24; the shortest contacts to naphthalene ring atoms are 3.474(5) Å to C2 and 3.383(5) Å to C3. A comparison of the seventeen ring torsion angles for **3** [23], with those of its ultimate precursor **1** shows that the ring torsion angles close to the aromatic ring are only modestly changed; and values (those for **1** given first) for C2-N1-C15-C16,

N1-C15-C16-C17, O3-C12-O5-C29, C12-O5-C29 C28 are −176.4°, −173.3(3)°; 63.6°, 59.8(4)°; −81.7°, −85.2(3)°; 65.9°, 66.0(4)°, respectively. The key 1,3-diol component of the ansa chain maintains its stereochemical integrity with values for C21-C22-C23-C24 of 63.2° and 55.0(4)°, along with accompanying values for C20-C21-C22-C23 of -172.1° and -176.0(3)°. For the structurally unaltered part of the ansa chain running from C21 to O5, the most dramatic change is found for torsion C25-C26-C27-C28, 56.0° and −171.6(3)°, respectively. Close to C18, massive changes are consequent upon double-bond migration, and for C16-C17-C18-C19, C17-C18-C19-C20, C18-C19-C20-C21, C19-C20-C21-C22 the corresponding values are: 36.5°, 146.4(3)°; −178.6°, −136.4(3)°; 117.4°, −1.2(5)°; −172.5°, 92.8(4)°.

A calculated overlay of compound **3**, Rifamycin O, **1** and Rifamycin S, **4** (CSD codes PUTDUD and PAFRAP, respectively) is shown in Figure 4. The overlay was computed based on all ten of the naphthalene core carbon atoms and yielded a r.m.s deviation of 0.0642Å for compound **3** and Rifamycin O, **1** and 0.0630Å for compound **3** and Rifamycin S, **4** [18]. Overlay figures for compound **3** and Rifamycin O, **1** and compound **3** and Rifamycin S, **4** [active conformation] can be found in the supplementary data. See below for details.

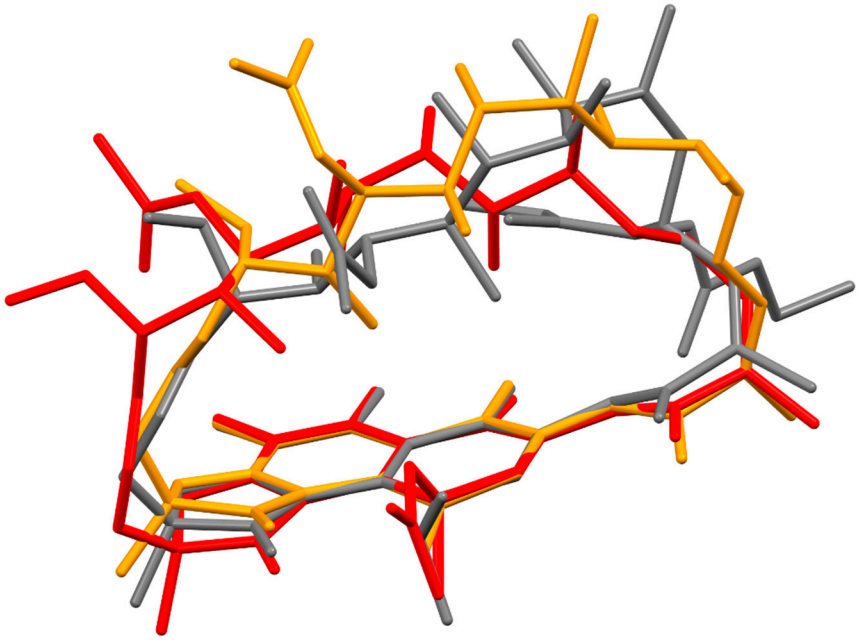

Figure 4. Overlay of compound **3** (grey), Rifamycin O (red) and Rifamycin S (orange) [active conformation]. See text for details.

5. Conclusions

New synthetic access to modified ansamycins is important for combatting mutant strains of bacterial pathogens. We have shown that whilst pure Rifamycin O is totally resistant to Diels–Alder addition, it reacts smoothly in an Alder-Ene process with diethyl azodicarboxylate and related azo compounds to give a new series of semi-synthetic rifamycins. The stereochemistry of the predominant product, **2**, of the addition reaction has been defined by conversion into a zwitterionic derivative **3** whose structure has been defined by single-crystal X-ray analysis, which established the absolute stereochemistry at C18 as having an *R* configuration, and a *Z* configuration at the introduced double bond between C19 and C20. A secondary product has been observed though not yet isolated and we have provisionally assigned to it a structure, isomeric with **2**, having an *S* configuration at C18 and a *trans* (*E*) double bond between C19 and C20. The potential anti-bacterial properties of **2** (and its isomer) and related compounds as well as those of zwitterionic **3** still remain to be determined. It is interesting to note that Rifamycin O has itself recently been found to show promise as an alternative anti-*Mycobacterium abscessus* agent [24].

Supplementary Materials: The following are available online at https://www.mdpi.com/article/10.3390/chemistry3030052/s1, Figure S1: Structure overlay for compound **3** and Rifamycin O, **1.** Figure S2: Structure overlay for compound **3** and Rifamycin S, **4.**

Author Contributions: Conceptualization, D.D.M. and J.H.G.; methodology, C.S.F., D.D.M. and J.H.G.; validation, C.S.F.; formal analysis, C.S.F. and D.D.M.; investigation, C.S.F., D.D.M. and J.H.G.; resources, C.S.F. and D.D.M.; data curation, C.S.F.; writing—original draft preparation, C.S.F. and D.D.M.; writing—review and editing, C.S.F. and D.D.M.; visualization, C.S.F. and D.D.M.; funding acquisition, D.D.M. All authors have read and agreed to the published version of the manuscript.

Funding: This research was funded Financial support from the Malaysia HIR MOHE, Grant No.F000009-21001 is gratefully acknowledged.

Data Availability Statement: The data is available from the CCDC program. CCDC 2045594 contains the supplementary crystallographic data for compound **3**, which can be obtained free of charge from The Cambridge Crystallographic Data Centre, see www.ccdc.cam.ac.uk/structures.

Acknowledgments: We thank F. Johnson (Stony Brook) for kindly providing a pure sample of Rifamycin O.

Conflicts of Interest: The authors declare that there are no conflicts of interest.

Sample Availability: Samples of the compounds are unavailable from the authors.

References

1. Floss, H.G.; Yu, T.-W. RifamycinMode of Action, Resistance, and Biosynthesis. *Chem. Rev.* **2005**, *105*, 621–632. [CrossRef]
2. Nigam, A.; Almabruk, K.H.; Saxena, A.; Yang, J.; Mukherjee, U.; Kaur, H.; Kohli, P.; Kumari, R.; Singh, P.; Zakharov, L.N.; et al. Modification of Rifamycin Polyketide Backbone Leads to Improved Drug Activity against Rifampicin-resistant Mycobacterium tuberculosis. *J. Biol. Chem.* **2014**, *289*, 21142–21152. [CrossRef]
3. Combrink, K.; Denton, D.A.; Harran, S.; Ma, Z.; Chapo, K.; Yan, D.; Bonventre, E.; Roche, E.D.; Doyle, T.B.; Robertson, G.T.; et al. New C25 carbamate rifamycin derivatives are resistant to inactivation by ADP-ribosyl transferases. *Bioorganic Med. Chem. Lett.* **2007**, *17*, 522–526. [CrossRef]
4. Dabbs, E.R.; Yazawa, K.; Mikami, Y.; Miyaji, M.; Morisaki, N.; Iwasaki, S.; Furihata, K. Ribosylation by mycobacterial strains as a new mechanism of rifampin inactivation. *Antimicrob. Agents Chemother.* **1995**, *39*, 1007–1009. [CrossRef]
5. Spanogiannopoulos, P.; Waglechner, N.; Koteva, K.; Wright, G.D. A rifamycin inactivating phosphotransferase family shared by environmental and pathogenic bacteria. *Proc. Natl. Acad. Sci. USA* **2014**, *111*, 7102–7107. [CrossRef]
6. Bacchi, A.; Pelizzi, G.; Nebuloni, M.; Ferrari, P. Comprehensive Study on Structure−Activity Relationships of Rifamycins: Discussion of Molecular and Crystal Structure and Spectroscopic and Thermochemical Properties of Rifamycin O. *J. Med. Chem.* **1998**, *41*, 2319–2332. [CrossRef] [PubMed]
7. Hoffmann, H.M.R. The Ene Reaction. *Angew. Chem. Int. Ed.* **1969**, *8*, 556–577. [CrossRef]
8. Singleton, D.A.; Hang, C. Isotope Effects and the Mechanism of Triazolinedione Ene Reactions. Aziridinium Imides Are Innocent Bystanders. *J. Am. Chem. Soc.* **1999**, *121*, 11885–11893. [CrossRef]
9. Cricchio, R.; Tamborini, G. New series of semisynthetic rifamycins. N-substituted derivatives of 4-amino-4-deoxyrifamycin SV. *J. Med. Chem.* **1971**, *14*, 721–723. [CrossRef] [PubMed]
10. Sheldrick, G.M. SHELXT—Integrated space-group and crystal-structure determination. *Acta Crystallogr. Sect. A Found. Adv.* **2015**, *71*, 3–8. [CrossRef] [PubMed]
11. Sheldrick, G.M. Crystal structure refinement with SHELXL. *Acta Crystallogr. Sect. C Struct. Chem.* **2015**, *71*, 3–8. [CrossRef]
12. Flack, H.D. On enantiomorph-polarity estimation. *Acta Crystallogr. Sect. A Found. Crystallogr.* **1983**, *39*, 876–881. [CrossRef]
13. Parsons, S.; Flack, H.D.; Wagner, T. Use of intensity quotients and differences in absolute structure refinement. *Acta Crystallogr. Sect. B Struct. Sci. Cryst. Eng. Mater.* **2013**, *69*, 249–259. [CrossRef] [PubMed]
14. Hooft, R.W.W.; Straver, L.H.; Spek, A.L. Determination of absolute structure using Bayesian statistics on Bijvoet differences. *J. Appl. Crystallogr.* **2008**, *41*, 96–103. [CrossRef] [PubMed]
15. Hooft, R.W.W.; Straver, L.H.; Spek, A.L. Probability plots based on Student'st-distribution. *Acta Crystallogr. Sect. A Found. Crystallogr.* **2009**, *65*, 319–321. [CrossRef]
16. Hooft, R.W.W.; Straver, L.H.; Spek, A.L. Using thet-distribution to improve the absolute structure assignment with likelihood calculations. *J. Appl. Crystallogr.* **2010**, *43*, 665–668. [CrossRef]
17. Spek, A.L.; Program PLATON. *A Multipurpose Crystallographic Tool. © 2021–2020*; Utrecht University: Utrecht, The Netherlands, 1980–2020.
18. Macrae, C.F.; Sovago, I.; Cottrell, S.J.; Galek, P.T.A.; McCabe, P.; Pidcock, E.; Platings, M.; Shields, G.P.; Stevens, J.S.; Towler, M.; et al. Mercury 4.0: From visualization to analysis, design and prediction. *J. Appl. Crystallogr.* **2020**, *53*, 226–235. [CrossRef]
19. Arora, S.K.; Arjunan, P. Molecular structure and conformation of rifamycin S, a potent inhibitor of DNA-dependent RNA polymerase. *J. Antibiot.* **1992**, *45*, 428–431. [CrossRef] [PubMed]

20. Bujnowski, K.; Synoradzki, L.; Darłak, R.C.; Zevaco, T.A.; Dinjus, E. Semi-synthetic zwitterionic rifamycins: A promising class of antibiotics; survey of their chemistry and biological activities. *RSC Adv.* **2016**, *6*, 114758–114772. [CrossRef]
21. Pyta, K.; Wicher, B.; Stefanska, J.; Przybylski, P.; Gdaniec, M. Intramolecular proton transfer impact on antibacterial properties of ansamycin antibiotic rifampicin and its new amino analogues. *Org. Biomol. Chem.* **2012**, *10*, 2385–2388. [CrossRef]
22. Wicher, B.; Pyta, K.; Przybylski, P.; Tykarska, E.; Gdaniec, M. Redetermination of rifampicin pentahydrate revealing a zwitterionic form of the antibiotic. *Acta Crystallogr. Sect. C Cryst. Struct. Commun.* **2012**, *68*, o209–o212. [CrossRef] [PubMed]
23. Bacchi, A.; Carcelli, M.; Pelizzi, G. Sampling rifamycin conformational variety by cruising through crystal forms: Implications for polymorph screening and for biological models. *New J. Chem.* **2008**, *32*, 1725–1735. [CrossRef]
24. Hanh, B.T.B.; Park, J.-W.; Kim, T.H.; Kim, J.-S.; Yang, C.-S.; Jang, K.; Cui, J.; Oh, D.-C.; Jang, J.; Rifamycin, O. An Alternative Anti-Mycobacterium abscessus Agent. *Molecules* **2020**, *25*, 1597. [CrossRef] [PubMed]